Published in final edited form as:
Biomacromolecules. 2013 November 11; 14(11): . doi:10.1021/bm401122q.

SDF-1α in Glycan Nanoparticles Exhibits Full Activity and Reduces Pulmonary Hypertension in Rats

Tao Yin[1,2], **Andrew R. Bader**[1], **Tim K. Hou**[1], **Bradley A. Maron**[1], **Derrick D. Kao**[1], **Ray Qian**[1], **Daniel S. Kohane**[3], **Diane E. Handy**[1], **Joseph Loscalzo**[1], and **Ying-Yi Zhang**[1,*]

[1]Department of Medicine, Brigham and Women's Hospital, and Harvard Medical School, Boston, MA

[2]Department of Cardiology, Xijing Hospital, The Fourth Military Medical University, China

[3]Laboratory for Drug Delivery and Biomaterials, Department of Anesthesiology, Division of Critical Care, Boston Children's Hospital, Boston, MA

Abstract

In order to establish a homing signal in the lung to recruit circulating stem cells for tissue repair, we formulated a nanoparticle, SDF-1α NP, by complexing SDF-1α with dextran sulfate and chitosan. The data show that SDF-1α was barely released from the nanoparticles over an extended period of time *in vitro* (3% in 7 days at 37°C); however, incorporated SDF-1α exhibited full chemotactic activity and receptor activation compared to its free form. The nanoparticles were not endocytosed after incubation with Jurkat cells. When aerosolized into the lungs of rats, SDF-1α NP displayed a greater retention time compared to free SDF-1α (64% vs. 2% remaining at 16 hr). In a rat model of monocrotaline-induced lung injury, SDF-1α NP, but not free form SDF-1α, was found to reduce pulmonary hypertension. These data suggest that the nanoparticle formulation protected SDF-1α from rapid clearance in the lung and sustained its biological function *in vivo*.

Keywords

CXCL12; glycosaminoglycan; internalization; FITC-SDF-1α

Introduction

Stem cell therapy has the potential to improve injury-related lung diseases, such as pulmonary hypertension, emphysema, and bronchopulmonary dysplasia. The difficulty with this therapy, however, is the challenge of targeting stem cells to an organ that is air-filled with diffuse and often heterogeneous disease lesions. Commonly used local injection methods for stem cell therapy is not possible. As an alternative approach, we sought to aerosolize SDF-1α in the lung to establish a homing signal in order to recruit circulating stem cells to the injured tissue.

SDF-1α has been known to play fundamental roles in stem cell homing. During embryonic development, SDF-1α mediates the homing and colonization of two critical populations of stem cells to their final destination organs: primordial germ cells to the gonad [1] and hematopoietic stem cells to the bone marrow [2]. In adulthood, SDF-1α maintains hematopoietic stem cells as well as other types of stem/progenitor cells in the bone

Correspondence to: Ying-Yi Zhang, Ph.D., Brigham and Women's Hospital, Harvard Medical School, 77 Avenue Louis Pasteur, NRB 0630, Boston, MA 02115, Phone : 617-525-4848, Fax : 617-525-4830, yyzhang@rics.bwh.harvard.edu.

marrow [3, 4]. Additionally, SDF-1α participates in tissue repair after injury by mobilizing stem cells from bone marrow to peripheral blood and recruiting these cells to the site of injury [5].

The homing function of SDF-1α is mediated by its chemoattractant activity. Indeed, SDF-1α is structurally related to a group of 50 small proteins, named chemotactic cytokines or chemokines [6]. In this superfamily, SDF-1α is referred to as CXCL12, and its receptors, CXCR4 and CXCR7. SDF-1α adopts the remarkably conserved tertiary structure as well as the heparin-binding sequence of the chemokine superfamily, which allow the chemokines to bind to cell surface glycosaminoglycans and subsequently form dimers or oligomers [7]. Chemokines in general mediate leukocyte trafficking; SDF-1α is no exception in this regard. It interacts with T-cells and monocytes in particular [8]. SDF-1α differs, however, from all other chemokines in that it is constitutively expressed in all tissue/organs (except in blood cells) [9, 10] and in that its expression is either unaffected or decreased (instead of stimulated) by inflammatory stimuli, such as lipopolysaccharide (LPS), IL-1, TNF-α, and IFN-γ [11, 12]. Tissue injury and hypoxia, by contrast, promote SDF-1α expression [13, 14]. Thus, the leukocyte chemotactic activity of SDF-1α is thought to play an important role in immune surveillance and in maintenance of tissue homeostasis [8, 15].

Based on its role in stem cell homing, SDF-1α has been administered to several animal disease models for the treatment of myocardial infarction (for review see [5]), spinal cord injury [16–18], stroke [19], skeletal muscle injury [20], bone and tendon damage [21, 22], and dermal wounds [23–25]. These studies showed that the SDF-1α administration improves tissue/cell function and angiogenesis, and reduces infiltration of inflammatory cells in the injured area. Different physical forms of SDF-1α were used in these studies. In the treatment of bone, spinal cord, and skeletal muscle injury, SDF-1α was infused in free form into the tissues by osmotic pump or by simple injection. In heart, tendon, and skin injury, SDF-1α has been delivered through bioengineered scaffolds, including nanofibers, PEGylated fibrin patches, knitted silk-collagen sponge scaffolds, alginated hydrogel patches, and collagen-glycosaminoglycan scaffold. Apparently, these methodologies have all resulted in sustained elevation in SDF-1α concentration in the injured area and produced beneficial effects after delivery. Their unique applications are related to the specific tissue environments of the damaged area.

For the purpose of lung delivery, in this study we chose to use a SDF-1α nanoparticle (SDF-1α NP) prepared by complexing SDF-1α with two charged glycans, dextran sulfate (DS) and chitosan (CS). The nanoparticle approach, which we have used previously [26], was preferred for two reasons. One is that free SDF-1α is known to be degraded readily in tissue by several proteases [27–30], while heparin-bound or dimerized SDF-1α has been shown to be resistant to protease digestion [31, 32]. DS has similar structural properties as those of heparin, and may, therefore, protect the delivered SDF-1α in the lung. The second reason is related to the structure of the airway, which branches by orthogonal bifurcation and becomes narrower while branching. The diameter of the alveolus/alveolar duct is reported to be 25–100 μm in rats [33, 34]. As the stem cell homing mechanism operates at the alveolar-capillary boundary, it is critical that the aerosolized SDF-1α complexes be small and sufficiently mobile to reach the target. The following report describes studies of a negatively-charged SDF-1α-dextran sulfate-chitosan NP with a diameter of ~700 nm. This study demonstrated that the incorporated SDF-1α was barely released from the particles *in vitro*, but exhibited full activities with regard to cell migration, receptor internalization, and downstream signaling pathway activation. A rat model of monocrotaline-induced pulmonary vascular injury and subsequent pulmonary hypertension was used to compare the effects of SDF-1α NP and free SDF-1α *in vivo*. It was found that the NP, but not free form SDF-1α, reduced the pulmonary

hypertension. These effects were consistent with rapid clearance of free SDF-1α in the lung after aerosol delivery, which was prevented by the glycan NP formulation.

Materials and Methods

Chitosan (MW range 50–190 kDa, 75–85% deacetylated), anti-smooth muscle cell α-actin monoclonal antibody, and AMD3100 were obtained from Sigma-Aldrich. UltraPure chitosan chloride (Approx. MW < 200 kDa, 75–90% deacetylated) was purchased from NovaMatrix (Protasan UP CL 113). Dextran sulfate, weight-average MW 500 kDa, was purchased from Fisher Scientific (#1585-100). UltraPure DNase/RNase-Free distilled water was obtained from Invitrogen. SDF-1α was prepared in our laboratory (see below), and also purchased from R&D Systems. Anti-phophoERK1/2 and anti-ERK antibodies were obtained from Cell Signaling. APC conjugated anti-CXCR4 antibody was purchased from BD biosciences. Monocrotaline was obtained from Trans World Chemicals, Inc. (Rockville, MD). MicroSprayer®Aerosolizer - Model IA-1B-R was purchased from Penn-Century, Inc. (Wyndmoor, PA). Fetal bovine serum was purchased from Atlanta Biologicals (# S11550). Bovine serum albumin (Probumin) was from Millipore (# 82-045-1). Chitosan fluorescein and chitosan rhodamine were obtained from Creative PEGWorks (Winston Salem, NC).

Preparation of recombinant human SDF-1α

The open reading frame of human SDF-1α cDNA was modified and the codon optimized for expression in *E.coli*. These modifications included deletion of the signal sequence (Asn2 to Gly21), and changing Pro23 codon CCC to CCA and Leu76 codon CTA to CTG. The optimized sequence was inserted into an expression vector, pET-11a (EMD), and subsequently used to transform an *E.coli* strain, BL21(DE) codon plus RP, obtained from Stratagene. The expression of SDF-1α was carried out in an autoinduction medium, Overnight Express™ Instant TB Medium, obtained from EMD. To purify SDF-1α, *E.coli* pellets from the expression culture were suspended in STE buffer (100 mM NaCl, 50 mM Tris HCl, pH 8.0, and 1 mM EDTA) containing 10% glycerol, 15% sucrose, and 0.1 mg/ml lysozyme. The suspension was incubated at room temperature for 2 hr with stirring and then mixed with 2%Triton X-100. The resulting lysate was sonicated and centrifuged at 16,000 x g for 30 min. SDF-1α inclusion bodies in the centrifugation pellet were washed with STE buffer plus 2% Triton X100 and then with STE buffer twice. SDF-1α was solubilized, refolded, and purified according to a previously described procedure [35]. The solubilizing solution contained 50 mM Tris HCl, pH 8.0, 6 M guanidine, and 10 mM DTT, and the refolding was carried out by dialysis against STE buffer containing 0.4 M arginine hydrochloride, 1 mM reduced glutathione, and 1 mM oxidized glutathione. The renatured SDF-1α was further purified with reverse-phase high-pressure liquid chromatography using a Source RPC 15 column (GE Healthcare Life Sciences).

Preparation of SDF-1α NPs

All reagents used in this preparation were dissolved in UltraPure Water (Invitrogen) and sterile filtered. SDF-1α NPs were prepared as previously described [26] with several modifications. Briefly, lyophilized SDF-1α was dissolved in 30 mM HEPES buffer and mixed with a specified volume of 1% DS. After 20 min stirring at 800 rpm, a specified volume of 0.1% chitosan (CS) was added. $ZnSO_4$ solution was subsequently added to a final concentration of 25 mM, and the reaction mixture was stirred for 30 min before 15% mannitol solution was added. The resulting SDF-1α-CS-DS particles were pelleted by centrifugation at 16,000 x g for 15 min at 4°C. The particles were washed three times with 5% mannitol, and stored at 4°C for further analysis. Two sources of CS were used in this study: chitosan (Sigma) and UltraPure chitosan chloride (NovaMatrix). The former was dissolved in 0.2% acetic acid/UltraPure water and the latter in UltraPure water. Both

solutions were adjusted to pH 5.5 and sterile filtered before use. There were no significant differences in particle size, entrapment efficiency, or inflammatory responses observed between the two forms, but the latter was used for the *in vivo* study described in this report.

To formulate SDF-1α NP containing fluorescein isothiocyanate (FITC)-conjugated SDF-1α (FITC-SDF-1α) and rhodamine-conjugated chitosan (rhodamine-chitosan), SDF-1α was stirred with DS for 20 min before addition of NHS-Fluorescein (Pierce # 46410). Binding of SDF-1α to DS before interaction with the amine-reactive fluorescence dye reduces the chance of blocking critical basic residues in the protein sequence that are directly involved in binding to CXCR4 (Lys1) and interaction with heparin/DS (Lys 24, Lys 27). The SDF-1α-DS mixture was adjusted to pH 8.5 with borate buffer, and NHS-Fluorescein was added at a molar ratio of 20:1 to SDF. After incubation in the dark for 1 h, the unbound dye was removed with Fluorescent Dye Removal Columns (Pierce, # 22858). The number of incorporated FITC was estimated by a fluorescence measurement against FITC standards (Pierce, # 46425). Approximately 3–5 fluorescein moieties were conjugated to each SDF-1α molecule. The fluorescent SDF-1α/DS complexes were subsequently incubated with rhodamine-chitosan, and followed by remaining steps in the NP preparation. The SDF-1α content and activity in the final fluorescent SDF-1α NPs were determined by methods described below.

To determine the particle size and zeta potential, SDF-1α particles were diluted in water and measured in ZetaPALS zeta potential analyzer (Brookhaven Instruments). The SDF-1α content in the particles was determined by SDS polyacrylamide gel electrophoresis (SDS PAGE) in combination with densitometry analysis. Briefly, SDF-1α particle suspensions were boiled in 1 x Laemmli sample buffer for 10 min with vortexing. The samples were then loaded to a 4–20% SDS gel (BioRad) and the gel run at 200 V for 25 min. The gels were stained with Coomassie blue using GelCode Blue stain reagent (Pierce). Densitometry analysis was performed using a VersaDoc imaging system and Quantity One image analysis software from BioRad. The quantity of SDF-1α in the particles was calculated against a standard curve constructed with soluble SDF-1α standards run in the same gel.

Migration assay

A cell migration assay (chemotaxis assay) was carried out using Costar polycarbonate Transwell inserts (pore size 5 μm, diameter 6.5 mm) placed in wells of a 24-well plate (Costar # 3421). Jurkat cells (5×10^5) were suspended in 100 μL Migration Medium [RPMI-1640 medium containing 0.5% bovine serum albumin (BSA, Sigma # A9576)] and added to a Transwell insert (top well). SDF-1α was diluted in 0.6 ml migration medium and added to a well in the 24 well plate (bottom well). Incubation was carried out at 37°C for 2 hr in a 5% CO_2 incubator. Cells that transmigrated into the bottom well were vigorously suspended and counted with a BD Accuri C6 flow cytometer equipped with a CFlow Plus program (BD Biosciences). Each sample was counted twice at a pre-set slow flow rate (14 μL/min) for 10 μL. For negative controls, the cells were added to the top wells but no SDF-1α in the bottom wells. For the input cell number, cells were added directly to the bottom well and counted with the migration samples. Migration was calculated as a percentage of the input cell number after subtraction of the numbers in negative controls. The subtraction of the negative control was avoided in Figure 5 in order to demonstrate the competition between forms of SDF-1α loaded in both top and bottom wells.

Assessing internalization of CXCR4 and SDF-1α NP

Jurkat cells were incubated with SDF-1α NPs in Migration Medium for 30 min at 37°C. The incubation mixture was centrifuged to separate cells from unbound NPs. The cells were washed once with Migration Medium and fixed at 4°C for 20 min with 4%

paraformaldehyde and 1% sucrose in PBS solution. The cells were subsequently permeabilized at 22°C for 5 min with 0.2% saponin, 1%BSA, and 1% sucrose in PBS solution, and immediately washed with PBS containing 1% BSA and 0.1% NaN3 (Staining Buffer). Antibody staining was performed at 4°C for 30 min with APC-conjugated anti-CD184 monoclonal antibody (BD Pharmingen # 555976, clone 12G5, for CXCR4 detection), and anti-fluorescein rabbit IgG (Alexa 488 conjugate, Invitrogen # A-11090, for amplifying FITC signals). The cells were washed with Staining Buffer and incubated with 1 μg/ml DAPI in PBS at 22°C for 5 min before loading on slides. Confocal laser scanning microscopy was performed with Zeiss LSM 700 system equipped with ZEN microscope software.

In vitro release study

SDF-1α NPs were suspended in Release Buffer containing 2.5% mannitol and 50% Dulbecco's phosphate-buffered saline without calcium and magnesium (D-PBS). (Note that the release buffer supports the stability of DS-CS NPs which are colloids of polyelectrolyte complexes.) The suspension was divided into 0.05 mL aliquots and rotated at 37°C on a Labquake Rotating Micro-Tube Mixer. At specified timepoints, the samples were removed and immediately centrifuged at 16,000 × g for 10 min at 4 °C. The supernatants and pellets were separated and stored at −20°C. The pellets were reconstituted with 0.05 mL of Release Buffer and examined with the supernatants using SDS PAGE. The quantity of the released SDF-1α was determined by ELISA using a kit from R&D systems. The activity of the released SDF-1α was measured by a Jurkat cell migration assay.

Animal studies

Sprague-Dawley male rats weighing 200–225 g were purchased from Charles River Laboratories, and were acclimated for 4 days in our animal facility. Animal studies were performed according to protocols approved by the Harvard Medical Area Standing Committee on Animals. Animals were maintained with unlimited food and water access, regular 12 hr light-dark cycle, no forced exercise, and in a generally pathogen-free environment.

Intratracheal aerosolization and analysis for lung tissue SDF-1α content

Rats were anesthetized with isoflurane and placed on a Tilting WorkStand (Hallowell EMC). The vocal cords of the animal were visualized with a specula-attached otoscope. A small amount of 2% lidocaine HCl jelly was applied to the vocal cords and surrounding vestibular folds. A sterilized MicroSprayer®Aerosolizer attached to a 0.5-ml gastight syringe was inserted into the trachea and advanced to ~1 cm above the bifurcation point. The aerosolized solution (0.25 mL) was delivery to the rat at the beginning of an inhalation cycle. At the specified time after delivery, lung tissue of the rats was harvested and frozen in liquid nitrogen. The tissue was homogenized in ice-cold homogenization buffer containing D-PBS, 2 mM EDTA, and 1% Protease Inhibitor Cocktail set III (Calbiochem #539134) using a Polytron homogenizer (Kenematica Model PT2100) at 22,000 rpm for 30 s for two cycles. The homogenate was divided into 0.5 mL aliquots and sonicated on ice for three cycles at 20% amplitude for 30 sec at a pulse frequency of 3 sec on and 1 sec off. The homogenates were centrifuged twice at 18,000 × g for 15 min at 4 °C. Supernatants were stored at −80 °C. The protein concentrations in the supernatants were determined by the BCA protein assay using bovine serum albumin as a standard. SDF-1α concentrations in the homogenate supernatants were determined by ELISA using reagents from R&D systems following the manufacturer's instructions.

Bronchoalveolar lavage (BAL)

Rats were euthanized by injection of ketamine (130 mg/kg) and xylazine (8 mg/kg) followed by exsanguination. An 18 gauge tubing adaptor was inserted into the trachea. D-PBS (5 mL) was gently flushed into and aspirated from the lungs, and the lavage repeated five times. The BAL fluids were combined and centrifuged at 500 × g for 10 min. The resulting cell pellet was suspended in 1 mL of 1 x RBC Lysis Buffer (eBiosciences) and incubated at room temperature for 5 min. The cells were pelleted again and resuspended in 1 ml D-PBS. The leukocyte number in the suspension was counted using a hemocytometer.

Right heart catheterization and histological analysis

Right heart catheterization was performed as described previously [36] with several modifications. Briefly, rats were anesthetized with ketamine (93 mg/kg) and xylazine (6.5 mg/kg), and the right jugular vein was dissected. A piece of PE-50 tubing with a shaped tip was inserted into the vein and advanced into the right ventricle. The tubing was connected to a Millar Pressure-Volume System (MPVS-400) through a Deltran® disposable blood pressure transducer (Utah Medical Products) and a bridge amplifier (ADInstrument). The pressure tracing was analyzed by PVAN data analysis software. Histological analyses of the rat lung tissues were performed as previously described [37]. Paraffin-embedded lung tissue sections (5 μm) were stained with hematoxylin and eosin (H&E staining) and with anti-smooth muscle α-actin antibody.

Statistics

Data are presented as mean ± standard error of mean (SEM). Statistical analysis was performed by one-way ANOVA and Tukey's multiple comparison test. $P < 0.05$ indicates statistical significance.

Results

Preparation of recombinant human SDF-1α

Owing to the large quantity of SDF-1α required for the present study, recombinant human SDF-1α was prepared in our laboratory. The protein was initially expressed in a baculovirus-insect cell expression system as we previously described [26], but the secreted SDF-1α was found at a low level in the culture medium. Only ~0.65 mg SDF-1α was purified from 1L expression culture. SDF-1α was subsequently expressed in an *E.coli* expression system, which gave a yield of 6–8 mg purified SDF-1α per liter of culture. In the *E.coli* expression system, the starting codon-translated methionine was retained at the N-terminus of SDF-1α. It was not removed after the purification, as previous reports indicated that N-terminal extension of methionine or glycine does not affect the activity of SDF-1α [35, 38, 39]. Indeed, compared to the insect cell-expressed SDF-1α and an *E.coli*-expressed SDF-1α with the N-terminal methionine removed (R&D Systems), the SDF-1α exhibited similar chemotactic activity (Fig. 1). The EC_{50}s of these purified SDF-1α were in the range of 0.14 – 0.61 ng/ml.

Formulation of SDF-1α NP

SDF-1α NPs were prepared by mixing SDF-1α with dextran sulfate (DS) and chitosan (CS). To obtain negatively charged particles with sizes between 200–800 nm and maximum SDF-1α entrapment, various SDF-1α/CS/DS ratios were investigated. As shown in Figure 2A, at fixed amounts of SDF-1α (40 μg) and DS (1 mg), varying CS/DS ratios of 0.2/1, 0.25/1, 0.33/1, and 0.5/1 resulted in particle sizes of 636 ± 15, 574 ± 34, 622 ± 17, and 1252 ± 95 nm, respectively. The particles in these preparations all exhibited negative zeta potentials, and no significant difference was observed among the groups (−40.8 to −43.6

mV, Fig. 2B). The entrapment efficiencies of SDF-1α in these preparations were also similar among the groups, ranging between 77–80% of initial input (Figs. 2C and 2D). Thus, CS/DS ratios of 0.25/1 and 0.33/1 were chosen for subsequent studies.

At fixed amounts of CS (0.33 mg) and DS (1 mg), varying SDF-1α quantities of 20, 40, 80, and 120 μg resulted in particles sizes of 585 ± 27, 640 ± 27, 705 ± 19, and 794 ± 60 nm, respectively (Fig. 3A). The increase in particle size correlated with the amount of SDF-1α added. No statistical differences were found in zeta potentials (−45.6 to −47.4 mV, Fig. 3B) or entrapment efficiencies (66–77%, Figs. 3C, 3D) of these preparations. The total amount of SDF-1α in the particles, therefore, was proportional to the initial input of the protein (Fig. 3E). A similar trend was found in preparations with CS/DS ratio of 0.25/1. At 20, 40, 80, and 120 μg SDF-α1 particles sizes were 591 ± 38, 635 ± 39, 697 ± 34, and 757 ± 37 nm, respectively. In the following studies, SDF-1α particles were prepared at ratios of SDF-1α/CS/DS of 0.04/0.33/1 (for *in vitro* study) or 0.08/0.33/1 (for *in vivo* delivery), and referred to as SDF-1α NPs.

In vitro release study

To investigate the rate of release of SDF-1α from the NPs, the particles were suspended in Release Buffer (2.5% mannitol and 50% D-PBS), divided into small aliquots, and rotated at 37°C for various periods of time. The released SDF-1α was separated from the NPs by centrifugation. The supernatants (contained released SDF-1α) and pellets (contained SDF-1α NP) were analyzed by SDS PAGE, ELISA, and migration assay. As shown in Figure 4A, SDF-1α in the supernatants collected between 0 hr and 7 days was barely detectable by Coomassie blue staining, while that in the pellets appeared to be unchanged throughout the incubation time. To quantify better the minimally released SDF-1α, ELISA was performed. As shown in Figure 4B, only 3.4% SDF-1α was released from the NPs after a 7-day incubation, and the amount released plateaued at 48 hrs. Nevertheless, the released SDF-1α retained its chemotactic activity as shown in the migration assay (Fig. 4C).

To better mimic the *in vivo* situation, the release of SDF-1α from the NPs was performed in Release Buffer containing 5, 10, or 20% fetal bovine serum (FBS), or 2 or 10 mg/ml bovine serum albumin (BSA). Incubations were carried out at 37°C for 24 h. As shown in Figures 4D and 4E, these conditions did not cause significant release of SDF-1α from the NPs.

The tight interaction of SDF-1α protein and DS polymer could be related to the ionic interactions between the molecules. To examine this type of interaction, SDF-1α NPs were incubated with 0.15, 0.3, 0.6, 1.2, or 2.4 M NaCl at 37°C for 30 min. As shown in Figure 4F, SDF-1α was detected in the supernatants of samples incubated with 1.2 and 2.4 M NaCl. These concentrations are equivalent to 8- to 16-fold of physiological ionic strength (150 mM). Thus the results show that SDF-1α is unlikely to dissociate from the NPs in a physiological fluid environment.

Chemotactic activity of NP-bound SDF-1α

The migration assay was initially performed to compare the activities of NP-bound and free SDF-1α. As shown in Figure 5A, the dose-response curves of the two forms of SDF-1α were superimposable. An inhibition study was then carried out in which AMD3100, a specific inhibitor for receptor CXCR4, was incubated with Jurkat cells prior to the migration assay. As shown in Figure 5B, AMD3100 inhibited the SDF-1α-induced migration dose-dependently and to the same degree for both forms of SDF-1α. Comparison of the chemotactic activities of the two forms of SDF-1α was further evaluated by a competition assay in which various concentrations of SDF-1α NP were added to the top wells (transwells) and a fixed concentration (3 ng/mL) of SDF-1α (free form, FF) was added to

the bottom wells. As shown in Figure 5C, SDF-1α NP inhibited the migration of Jurkat cells toward the bottom wells at concentrations ≥ 3.2 ng/mL. Thus SDF-1α NP was able to compete for migration of Jurkat cells induced by the same concentration of free SDF-1α.

SDF-1α binding to CXCR4 is known to activate several downstream signaling pathways, including MAP kinase P42/44 or ERK1/2-dependent pathways [40]. ERK activation results in cell proliferation which is different from other CXCR4 activated pathways involving cytoskeleton rearrangement and migration. The effect of the two forms of SDF-1α on the activation of ERK1/2 was examined. As shown in Figure 6, the free SDF-1α and SDF-1α NP activated ERK1/2 similarly, both in a time course, (Fig. 6A) and dose-dependence (Fig. 6B).

Activation of CXCR4 by SDF-1α is also known to cause polarization and internalization of the receptor [41, 42]. To compare the effect of the two forms of SDF-1α in CXCR4 activation and intracellular translocation, Jurkat cells were treated with both forms of SDF-1α for 30 min and stained with a fluorescent conjugated anti-CXCR4 antibody. The localization of CXCR4 was examined by confocal microscopy. As shown in Figure 7, the two forms of SDF-1α caused similar CXCR4 polarization and internalization with no distinct morphological differences. Thus, in all the assays performed above, the SDF-1α NP exhibited the same activities as that of free form SDF-1α.

Analyses of Internalization of SDF-1α NP

In order to examine the localization of SDF-1α NPs after interaction with Jurkat cells, fluorescein-conjugated CS (FITC-CS) was used to prepare SDF-1α NPs instead of CS. The cells were stained for CXCR4 after the incubation in order to confirm the receptor activation. The localization of SDF-1α NP was examined by confocal laser scanning microscopy. The top panel in Figure 8 shows the confocal images of cells incubated with 10 –10,000 ng/ml SDF-1α NPs (concentrations normalized to SDF-1α). The FITC fluorescence was found on the surface of the cells that were incubated with 1,000 and 10,000 ng/ml SDF-1α NPs, but not in those incubated with the lower concentrations. The CXCR4 receptor, however, was activated in all the samples, indicating that interactions of SDF-1α NPs with the cells had taken place. No FITC fluorescence was present in the intracellular space of the cells. An anti-FITC antibody was used to amplify the FITC signal to detect the potentially bound SDF-1α NP in the low concentration samples, but no additional signal was found. Thus, these images indicated that the SDF-1α NPs were not endocytosed by the cells. Furthermore, the particles had limited retention on the cell surface, as the majority of the fluorescent NPs were washed away following the incubation.

To determine the distribution of SDF-1α, NPs containing FITC-SDF-1α and rhodamine-chitosan were used for interaction with Jurkat cells. The cells were stained with an anti-CXCR4 and an anti-FITC antibody (APC and Alexa 488 conjugated, respectively) after the incubation and subjected to confocal microscopic analysis. As shown in the lower panel of Figure 8, the rhodamine (chitosan) and FITC (SDF-1α) signals were colocalized on the cell surface, indicating that the components of the particles remained associated, and the particles were not endocytosed by the cells. A trace amount of SDF-1α (FITC label) was colocalized with the internalized CXCR4, which is consistent with a previous report demonstrating a minimal and a dramatic internalization of SDF-1α during interaction with CXCR4 and CXCR7, respectively [43].

In vivo inflammatory response analysis

Free SDF-1α or SDF-1α NP was next aerosolized into the lungs of rats in order to examine potential inflammatory responses caused by the delivery. Bronchoalveolar lavage (BAL)

was performed to access leukocyte infiltration in the lung at 24 or 48 hrs after the SDF-1α delivery. As shown in Figure 9A, rats received SDF-1α at doses of 20, 40, or 80 μg/rat had the same BAL leukocyte counts as those treated with D-PBS. Thus, SDF-1α at the high doses did not induce a significant inflammatory response in the lung. A comparison of the responses was then carried out in rats treated with aerosolized control NPs (made with CS and DS only), 15 μg SDF-1α, 15 μg SDF-1α NP, or LPS. As shown in Figure 9B, no statistical differences were found among the untreated rats and the rats treated with NP, SDF-1α, or SDF-1α NP, although the average nucleated cell counts in the SDF-1αNP-treated lung was slightly higher (~2-fold) than of that of the controls. Lipopolysaccharide, a positive control, caused more than 60-fold greater leukocyte infiltration compared to the controls.

In vivo retention time

To determine *in vivo* retention times of aerosolized SDF-1α or SDF-1α NP, lung tissues were harvested at 0, 1, 3, 5, 8, 16, 24, 48, and 72 hr after delivery. Supernatants of tissue homogenates were prepared, and the SDF-1α content was determined using ELISA. SDF-1α concentrations in the lung tissue samples were compared to those collected at 0 hr (immediately after delivery) and plotted as a percentage of 0 hr content. As shown in Figure 10, the SDF-1α content in the lung decayed in an exponential pattern. The half-life of the decay was 3.2 hr for SDF-1α and 20 hr for SDF-1α NP, with decay constants of 0.2146 hr^{-1} and 0.0345 hr^{-1}, respectively. The calculated decay plateaued at 2.2% for SDF-1α and 29% for the SDF-1α NP, corresponding to 16 hr and 72 hr, respectively, after the delivery of the protein to the rat lungs.

Effect in a rat model of lung injury and pulmonary hypertension

To determine whether aerosolized SDF-1α or SDF-1α NP is functional *in vivo*, a monocrotaline (MCT) rat model was employed. Intraperitoneal-injected MCT is known to be metabolized in rat liver to an active form, which, upon release into circulation, causes damage to the pulmonary vascular endothelium. The initial endothelial injury triggers a cascade of responses in the subsequent few weeks, which results in a muscularization or thickening of vessel walls of small/precapillary pulmonary arterioles and narrowing/occlusion of the vessel lumen [44]. These changes lead to an increase in pulmonary vascular resistance, and, thus, pulmonary hypertension. To examine the effect of SDF-1α in this rat model, rats were injected with MCT at day 0. At day 3 (after the pulmonary endothelial injury occurred), 15 μg SDF-1α in free or NP form were aerosolized into the lungs of rats. At day 21 (when the elevation of pulmonary artery pressure approached its highest values), right heart catheterization was performed to assess right ventricular systolic pressure (RVSP, which equals pulmonary artery systolic pressure in the absence of pulmonic valve disease). Lung tissue samples were collected after the catheterization to examine the histological changes in pulmonary vessels in the rats. As shown in Figure 11A, the average RVSP in the rats with no treatment (NoTx), or treated with MCT only, MCT + SDF-1α, and MCT + SDF-1α NP were 27 ± 0.8, 84 ± 4, 87 ± 4, and 69 ± 5 mmHg (M ± SEM), respectively. Thus, all MCT treated groups had elevated pulmonary pressure compared to the untreated group, and there was no statistical difference between the MCT only and the MCT+SDF-1α-treated groups. The MCT+SDF-1α NP-treated rats, however, had significant reduced pressure compared to the MCT groups. To confirm the reduced pulmonary artery pressure observed in the SDF-1α NP-treatment group resulted from a decrease in pulmonary vascular remodeling, immunohistochemical staining was carried out in four lung tissue samples from each group that exhibited RVSP below the average value of the group. Representative micrographs of the anti-smooth muscle α-actin antibody-stained sections are shown in Figure 11B, and counts of the muscularized precapillary vessels (diameter <50 μm) are shown in Figure 11C. These data demonstrated that SDF-1α NP-treated rats had both a

reduced total number of muscularized precapillary vessels and decreased thickness of the vessel walls. The overall analyses suggested a beneficial effect of SDF-1α NP in the rat model of pulmonary hypertension.

Discussion

The SDF-1α NP prepared in this study differs from many other nanoparticles in that the incorporated SDF-1α was not spontaneously released over the time *in vitro*. It is, thus, debatable whether the NP can exert a biological function through a sustained release mechanism that is expected for many other bioengineered particles/scaffolds. While the phenomenon was unexpected, it posed questions as to whether the incorporated SDF-1α is active without release, and whether the SDF-1α NP is functional *in vivo*. For this reason, we carried out an extended analysis to compare the activities of SDF-1α in its free and NP-incorporated forms. The chemotactic activities of the two forms of SDF-1α were examined in three different ways: a standard migration assay, a receptor inhibition assay (using AMD3100), and a competition assay (between the free and NP forms). The activation of receptor CXCR4 by the two forms of SDF-1α was visualized by confocal microscopic imaging. A downstream signaling pathway (ERK pathway) that mediates the cell survival and growth function of SDF-1α was examined by time course and dose response analyses. In all these assays, the NP-incorporated SDF-1α exhibited the same activity as its free form.

A literature search was carried out to understand why the NP-bound SDF-1α was not released, and yet able to exert full biological activity. It showed that this phenomenon is related to the intrinsic glycosaminoglycan-binding property of SDF-1α. Dextran sulfate (DS) used in the NP preparation has a similar structure as that of heparin or certain domains in heparan sulfate (Fig. 12). These are heavily sulfated and negatively charged polysaccharides and the major glycosaminoglycan forms. Previous studies have shown that SDF-1α has a heparin-binding site at Lys24-His25-Leu26-Lys27 (BBXB) and binds to heparin with high affinity (38 nM) [45]. The heparin binding of SDF-1α does not overlap with its receptor-binding site, which is at the N-terminus of the protein with the first two residues (Lys1-Pro2) directly involved in activation of CXCR4 [38]. Furthermore, studies of the heparin- and receptor-binding sites of SDF-1α suggested that glycosaminoglycan binding is crucial to the function of the protein [7, 46]: it facilitates chemokine tethering on the cell surface and leads to high local concentration. Using solid phase-bound SDF-1α systems, studies have shown that a spatial gradient is not necessary for the chemotactic activity of SDF-1α and certain other chemokines[41, 47]. The redistribution of CXCR4 to the leading edge of cells, thereby inducing polarization of the receptor, was proposed to determine the direction of the cell migration[41]. Whether a soluble gradient is relevant to the function of chemokines *in vivo* has been questioned, as chemokines direct leukocyte trafficking on the surface of endothelium facing blood flow[41, 47]. SDF-1α-induced internalization of CXCR4 and polarized redistribution of the receptor have been shown in several other studies [42, 48, 49].

In the present study, the same concentration of SDF-1α in free or NP form was used to compare the activities of the protein. Stoichiometrically, the number of free SDF-1α molecules in the incubation medium was greater than that of NPs. If the NPs were firmly attached to the cell surface once interacting with CXCR4, the frequency of concentration-dependent collisions would be significantly less, as would activities of SDF-1α NP. The dose-dependent images shown in Figure 8, top panel, suggest that this is not the case, as the majority of SDF-1α NPs were washed away after the incubation. The little attachment of the particles to the cells, likely due to an electrostatic repulsion between the negatively charged cell surface and the NPs, would allow multiple interactions between the SDF-1α NPs and CXCR4 molecules.

Investigating the correlation between surface charges of nanoparticles and their cellular uptake rate, previous studies have demonstrated that positively charged particles are more susceptible to cellular uptake than negatively charged ones [50, 51]. Positively charged and small rigid NPs (eg. polystyrene NP, 20–120 nm) can even translocate across alveolar epithelium, occurring at a flux rate ~65 times faster than that of negatively charged ones (see [52] and references therein). The present study showed that SDF-1α NPs were not internalized by Jurkat cells (Fig 8, lower panel). Avoiding endocytosis could help retain active SDF-1α NP delivered to the lung and minimize inflammatory responses against the particles.

By not being released from the NPs and exerting full chemotactic activity, the incorporated SDF-1α could serve as a stationary "homing" factor to attract mobilized stem cells. Several possible scenarios, however, can occur after the delivery of SDF-1α NPs to the lung. The NPs, which are colloids of polyelectrolyte complexes[53], can collapse after contacting the pulmonary epithelium over the time. SDF-1α in the NP matrix could exchange to the extracellular matrix, which is rich in negatively-charged glycosaminoglycans. In addition, SDF-1α or the matrix molecules of the NPs, dextran sulfate and chitosan, can be degraded in the lung. To compare the overall effect, we delivered free and NP-bound SDF-1α to the lungs of rats which were treated with MCT. An early time point after the MCT injury was chosen (day 3 after injection), as the acute injury provides other factors required for stem cell homing, including mobilization of bone marrow progenitor/stem cells and changes in permeability of the alveolar-capillary barrier. The data showed that SDF-1α NP, but not free SDF-1α, has a beneficial effect in reducing the pulmonary hypertension development after the MCT injury. The different effect of the two forms of SDF-1α is apparently related to their different retention times in the lung. A persistent homing signal would be more efficient than a relatively transient signal in recruiting low levels of circulating stem/progenitor cells. Furthermore, SDF-1α has been known to facilitate the survival and growth of stem cells by activating Akt and ERK1/2 pathways through CXCR4 activation[40, 54, 55].

Conclusion

In order to establish a homing signal in the lung to recruit circulating stem cells for tissue regeneration, this study formulated SDF-1α-DS-CS nanoparticles (SDF-1α NP) and examined the activities of the particles *in vitro* and *in vivo*. The *in vitro* studies showed that SDF-1α was barely released from the particles over an extended period of time (3% over 7 days at 37°C), and that particle-bound SDF-1α had the same activities as that of free SDF-1α. When aerosolized into the lungs of rats, SDF-1α NP exhibited greater retention time than that of free SDF-1α ($t_{1/2}$ = 20 hr, and 3.2 hr, respectively; 29% remaining after 72 hr vs. 2% after 16 hr, respectively). The aerosolized SDF-1α NPs, but not free form SDF-1α, reduced pulmonary artery pressure in monocrotaline-treated rats. These data indicate that SDF-1α NPs fit to the criteria for a desired homing signal in the lung. The rat pulmonary hypertension study indicated a potential use for SDF-1α NP in the treatment of injury-related pulmonary diseases.

Acknowledgments

This work was supported by NIH Grants: HL61795, HL48743, HL107192, 070819, and HL108630. We thank Stephanie Tribuna, Julia Wang, Justin E. Tribuna, and Shuangtian Li for assistance in the preparation of this manuscript.

References

1. Doitsidou M, Reichman-Fried M, Stebler J, Koprunner M, Dorries J, Meyer D, Esguerra CV, Leung T, Raz E. Guidance of primordial germ cell migration by the chemokine SDF-1. Cell. 2002; 111(5): 647–59. [PubMed: 12464177]
2. Ara T, Tokoyoda K, Sugiyama T, Egawa T, Kawabata K, Nagasawa T. Long-term hematopoietic stem cells require stromal cell-derived factor-1 for colonizing bone marrow during ontogeny. Immunity. 2003; 19(2):257–67. [PubMed: 12932359]
3. Rankin SM. Chemokines and adult bone marrow stem cells. Immunology letters. 2012; 145(1–2): 47–54. [PubMed: 22698183]
4. Sharma M, Afrin F, Satija N, Tripathi RP, Gangenahalli GU. Stromal-derived factor-1/CXCR4 signaling: indispensable role in homing and engraftment of hematopoietic stem cells in bone marrow. Stem cells and development. 2011; 20(6):933–46. [PubMed: 21186999]
5. Ghadge SK, Muhlstedt S, Ozcelik C, Bader M. SDF-1alpha as a therapeutic stem cell homing factor in myocardial infarction. Pharmacology & therapeutics. 2011; 129(1):97–108. [PubMed: 20965212]
6. Luster AD. Chemokines--chemotactic cytokines that mediate inflammation. The New England journal of medicine. 1998; 338(7):436–45. [PubMed: 9459648]
7. Proudfoot AE. The biological relevance of chemokine-proteoglycan interactions. Biochemical Society transactions. 2006; 34(Pt 3):422–6. [PubMed: 16709177]
8. Bleul CC, Fuhlbrigge RC, Casasnovas JM, Aiuti A, Springer TA. A highly efficacious lymphocyte chemoattractant, stromal cell-derived factor 1 (SDF-1). The Journal of experimental medicine. 1996; 184(3):1101–9. [PubMed: 9064327]
9. Shirozu M, Nakano T, Inazawa J, Tashiro K, Tada H, Shinohara T, Honjo T. Structure and chromosomal localization of the human stromal cell-derived factor 1 (SDF1) gene. Genomics. 1995; 28(3):495–500. [PubMed: 7490086]
10. Tashiro K, Tada H, Heilker R, Shirozu M, Nakano T, Honjo T. Signal sequence trap: a cloning strategy for secreted proteins and type I membrane proteins. Science. 1993; 261(5121):600–3. [PubMed: 8342023]
11. Fedyk ER, Jones D, Critchley HO, Phipps RP, Blieden TM, Springer TA. Expression of stromal-derived factor-1 is decreased by IL-1 and TNF and in dermal wound healing. Journal of immunology. 2001; 166(9):5749–54.
12. Murdoch C. CXCR4: chemokine receptor extraordinaire. Immunological reviews. 2000; 177:175–84. [PubMed: 11138774]
13. Ceradini DJ, Kulkarni AR, Callaghan MJ, Tepper OM, Bastidas N, Kleinman ME, Capla JM, Galiano RD, Levine JP, Gurtner GC. Progenitor cell trafficking is regulated by hypoxic gradients through HIF-1 induction of SDF-1. Nature medicine. 2004; 10(8):858–64.
14. Pillarisetti K, Gupta SK. Cloning and relative expression analysis of rat stromal cell derived factor-1 (SDF-1)1: SDF-1 alpha mRNA is selectively induced in rat model of myocardial infarction. Inflammation. 2001; 25(5):293–300. [PubMed: 11820456]
15. Karin N. The multiple faces of CXCL12 (SDF-1alpha) in the regulation of immunity during health and disease. Journal of leukocyte biology. 2010; 88(3):463–73. [PubMed: 20501749]
16. Jaerve A, Schiwy N, Schmitz C, Mueller HW. Differential effect of aging on axon sprouting and regenerative growth in spinal cord injury. Experimental neurology. 2011; 231(2):284–94. [PubMed: 21806987]
17. Opatz J, Kury P, Schiwy N, Jarve A, Estrada V, Brazda N, Bosse F, Muller HW. SDF-1 stimulates neurite growth on inhibitory CNS myelin. Molecular and cellular neurosciences. 2009; 40(2):293–300. [PubMed: 19084600]
18. Zendedel A, Nobakht M, Bakhtiyari M, Beyer C, Kipp M, Baazm M, Joghataie MT. Stromal cell-derived factor-1 alpha (SDF-1alpha) improves neural recovery after spinal cord contusion in rats. Brain research. 2012; 1473:214–26. [PubMed: 22842524]
19. Shyu WC, Lin SZ, Yen PS, Su CY, Chen DC, Wang HJ, Li H. Stromal cell-derived factor-1 alpha promotes neuroprotection, angiogenesis, and mobilization/homing of bone marrow-derived cells in stroke rats. The Journal of pharmacology and experimental therapeutics. 2008; 324(2):834–49. [PubMed: 18029549]

20. Brzoska E, Kowalewska M, Markowska-Zagrajek A, Kowalski K, Archacka K, Zimowska M, Grabowska I, Czerwinska AM, Czarnecka-Gora M, Streminska W, Janczyk-Ilach K, Ciemerych MA. Sdf-1 (CXCL12) improves skeletal muscle regeneration via the mobilisation of Cxcr4 and CD34 expressing cells. Biology of the cell / under the auspices of the European Cell Biology Organization. 2012; 104(12):722–37. [PubMed: 22978573]
21. Fujio M, Yamamoto A, Ando Y, Shohara R, Kinoshita K, Kaneko T, Hibi H, Ueda M. Stromal cell-derived factor-1 enhances distraction osteogenesis-mediated skeletal tissue regeneration through the recruitment of endothelial precursors. Bone. 2011; 49(4):693–700. [PubMed: 21741502]
22. Shen W, Chen X, Chen J, Yin Z, Heng BC, Chen W, Ouyang HW. The effect of incorporation of exogenous stromal cell-derived factor-1 alpha within a knitted silk-collagen sponge scaffold on tendon regeneration. Biomaterials. 2010; 31(28):7239–49. [PubMed: 20615544]
23. Henderson PW, Singh SP, Krijgh DD, Yamamoto M, Rafii DC, Sung JJ, Rafii S, Rabbany SY, Spector JA. Stromal-derived factor-1 delivered via hydrogel drug-delivery vehicle accelerates wound healing in vivo. Wound repair and regeneration : official publication of the Wound Healing Society [and] the European Tissue Repair Society. 2011; 19(3):420–5.
24. Rabbany SY, Pastore J, Yamamoto M, Miller T, Rafii S, Aras R, Penn M. Continuous delivery of stromal cell-derived factor-1 from alginate scaffolds accelerates wound healing. Cell transplantation. 2010; 19(4):399–408. [PubMed: 19995484]
25. Sarkar A, Tatlidede S, Scherer SS, Orgill DP, Berthiaume F. Combination of stromal cell-derived factor-1 and collagen-glycosaminoglycan scaffold delays contraction and accelerates reepithelialization of dermal wounds in wild-type mice. Wound repair and regeneration : official publication of the Wound Healing Society [and] the European Tissue Repair Society. 2011; 19(1): 71–9.
26. Lauten EH, VerBerkmoes J, Choi J, Jin R, Edwards DA, Loscalzo J, Zhang YY. Nanoglycan complex formulation extends VEGF retention time in the lung. Biomacromolecules. 2010; 11(7): 1863–72. [PubMed: 20575564]
27. Davis DA, Singer KE, De La Luz Sierra M, Narazaki M, Yang F, Fales HM, Yarchoan R, Tosato G. Identification of carboxypeptidase N as an enzyme responsible for C-terminal cleavage of stromal cell-derived factor-1alpha in the circulation. Blood. 2005; 105(12):4561–8. [PubMed: 15718415]
28. Durinx C, Lambeir AM, Bosmans E, Falmagne JB, Berghmans R, Haemers A, Scharpe S, De Meester I. Molecular characterization of dipeptidyl peptidase activity in serum: soluble CD26/dipeptidyl peptidase IV is responsible for the release of X-Pro dipeptides. European journal of biochemistry / FEBS. 2000; 267(17):5608–13. [PubMed: 10951221]
29. Herrera C, Morimoto C, Blanco J, Mallol J, Arenzana F, Lluis C, Franco R. Comodulation of CXCR4 and CD26 in human lymphocytes. The Journal of biological chemistry. 2001; 276(22): 19532–9. [PubMed: 11278278]
30. McQuibban GA, Butler GS, Gong JH, Bendall L, Power C, Clark-Lewis I, Overall CM. Matrix metalloproteinase activity inactivates the CXC chemokine stromal cell-derived factor-1. The Journal of biological chemistry. 2001; 276(47):43503–8. [PubMed: 11571304]
31. Sadir R, Imberty A, Baleux F, Lortat-Jacob H. Heparan sulfate/heparin oligosaccharides protect stromal cell-derived factor-1 (SDF-1)/CXCL12 against proteolysis induced by CD26/dipeptidyl peptidase IV. The Journal of biological chemistry. 2004; 279(42):43854–60. [PubMed: 15292258]
32. Takekoshi T, Ziarek JJ, Volkman BF, Hwang ST. A locked, dimeric CXCL12 variant effectively inhibits pulmonary metastasis of CXCR4-expressing melanoma cells due to enhanced serum stability. Molecular cancer therapeutics. 2012; 11(11):2516–25. [PubMed: 22869557]
33. Hyde DM, Tyler NK, Putney LF, Singh P, Gundersen HJ. Total number and mean size of alveoli in mammalian lung estimated using fractionator sampling and unbiased estimates of the Euler characteristic of alveolar openings. The anatomical record Part A, Discoveries in molecular, cellular, and evolutionary biology. 2004; 277(1):216–26.
34. Moreci AP, Norman JC. Measurements of alveolar sac diameters by incident-light photomicrography. Effects of positive-pressure respiration The Annals of thoracic surgery. 1973; 15(2):179–86.

35. Kofuku Y, Yoshiura C, Ueda T, Terasawa H, Hirai T, Tominaga S, Hirose M, Maeda Y, Takahashi H, Terashima Y, Matsushima K, Shimada I. Structural basis of the interaction between chemokine stromal cell-derived factor-1/CXCL12 and its G-protein-coupled receptor CXCR4. The Journal of biological chemistry. 2009; 284(50):35240–50. [PubMed: 19837984]
36. Jones JE, Mendes L, Rudd MA, Russo G, Loscalzo J, Zhang YY. Serial noninvasive assessment of progressive pulmonary hypertension in a rat model. American journal of physiology Heart and circulatory physiology. 2002; 283(1):H364–71. [PubMed: 12063310]
37. Jones JE, Walker JL, Song Y, Weiss N, Cardoso WV, Tuder RM, Loscalzo J, Zhang YY. Effect of 5-lipoxygenase on the development of pulmonary hypertension in rats. American journal of physiology Heart and circulatory physiology. 2004; 286(5):H1775–84. [PubMed: 14726295]
38. Crump MP, Gong JH, Loetscher P, Rajarathnam K, Amara A, Arenzana-Seisdedos F, Virelizier JL, Baggiolini M, Sykes BD, Clark-Lewis I. Solution structure and basis for functional activity of stromal cell-derived factor-1; dissociation of CXCR4 activation from binding and inhibition of HIV-1. The EMBO journal. 1997; 16(23):6996–7007. [PubMed: 9384579]
39. Holmes WD, Consler TG, Dallas WS, Rocque WJ, Willard DH. Solution studies of recombinant human stromal-cell-derived factor-1. Protein expression and purification. 2001; 21(3):367–77. [PubMed: 11281710]
40. Kucia M, Jankowski K, Reca R, Wysoczynski M, Bandura L, Allendorf DJ, Zhang J, Ratajczak J, Ratajczak MZ. CXCR4-SDF-1 signalling, locomotion, chemotaxis and adhesion. Journal of molecular histology. 2004; 35(3):233–45. [PubMed: 15339043]
41. Pelletier AJ, van der Laan LJ, Hildbrand P, Siani MA, Thompson DA, Dawson PE, Torbett BE, Salomon DR. Presentation of chemokine SDF-1 alpha by fibronectin mediates directed migration of T cells. Blood. 2000; 96(8):2682–90. [PubMed: 11023498]
42. van Buul JD, Voermans C, van Gelderen J, Anthony EC, van der Schoot CE, Hordijk PL. Leukocyte-endothelium interaction promotes SDF-1-dependent polarization of CXCR4. The Journal of biological chemistry. 2003; 278(32):30302–10. [PubMed: 12766157]
43. Luker KE, Steele JM, Mihalko LA, Ray P, Luker GD. Constitutive and chemokine-dependent internalization and recycling of CXCR7 in breast cancer cells to degrade chemokine ligands. Oncogene. 2010; 29(32):4599–610. [PubMed: 20531309]
44. Gomez-Arroyo JG, Farkas L, Alhussaini AA, Farkas D, Kraskauskas D, Voelkel NF, Bogaard HJ. The monocrotaline model of pulmonary hypertension in perspective. American journal of physiology Lung cellular and molecular physiology. 2012; 302(4):L363–9. [PubMed: 21964406]
45. Amara A, Lorthioir O, Valenzuela A, Magerus A, Thelen M, Montes M, Virelizier JL, Delepierre M, Baleux F, Lortat-Jacob H, Arenzana-Seisdedos F. Stromal cell-derived factor-1alpha associates with heparan sulfates through the first beta-strand of the chemokine. The Journal of biological chemistry. 1999; 274(34):23916–25. [PubMed: 10446158]
46. Laguri C, Arenzana-Seisdedos F, Lortat-Jacob H. Relationships between glycosaminoglycan and receptor binding sites in chemokines-the CXCL12 example. Carbohydrate research. 2008; 343(12):2018–23. [PubMed: 18334249]
47. Proudfoot AE, Handel TM, Johnson Z, Lau EK, LiWang P, Clark-Lewis I, Borlat F, Wells TN, Kosco-Vilbois MH. Glycosaminoglycan binding and oligomerization are essential for the in vivo activity of certain chemokines. Proceedings of the National Academy of Sciences of the United States of America. 2003; 100(4):1885–90. [PubMed: 12571364]
48. Nieto M, Frade JM, Sancho D, Mellado M, Martinez AC, Sanchez-Madrid F. Polarization of chemokine receptors to the leading edge during lymphocyte chemotaxis. The Journal of experimental medicine. 1997; 186(1):153–8. [PubMed: 9207004]
49. Vicente-Manzanares M, Montoya MC, Mellado M, Frade JM, del Pozo MA, Nieto M, de Landazuri MO, Martinez AC, Sanchez-Madrid F. The chemokine SDF-1alpha triggers a chemotactic response and induces cell polarization in human B lymphocytes. European journal of immunology. 1998; 28(7):2197–207. [PubMed: 9692889]
50. Morachis JM, Mahmoud EA, Almutairi A. Physical and chemical strategies for therapeutic delivery by using polymeric nanoparticles. Pharmacological reviews. 2012; 64(3):505–19. [PubMed: 22544864]

51. Yue ZG, Wei W, Lv PP, Yue H, Wang LY, Su ZG, Ma GH. Surface charge affects cellular uptake and intracellular trafficking of chitosan-based nanoparticles. Biomacromolecules. 2011; 12(7): 2440–6. [PubMed: 21657799]

52. Fazlollahi F, Kim YH, Sipos A, Hamm-Alvarez SF, Borok Z, Kim KJ, Crandall ED. Nanoparticle translocation across mouse alveolar epithelial cell monolayers: Species-specific mechanisms. Nanomedicine : nanotechnology, biology, and medicine. 2013; 9(6):786–94.

53. Schatz C, Domard A, Viton C, Pichot C, Delair T. Versatile and efficient formation of colloids of biopolymer-based polyelectrolyte complexes. Biomacromolecules. 2004; 5(5):1882–92. [PubMed: 15360302]

54. Cencioni C, Capogrossi MC, Napolitano M. The SDF-1/CXCR4 axis in stem cell preconditioning. Cardiovascular research. 2012; 94(3):400–7. [PubMed: 22451511]

55. Guo Y, Hangoc G, Bian H, Pelus LM, Broxmeyer HE. SDF-1/CXCL12 enhances survival and chemotaxis of murine embryonic stem cells and production of primitive and definitive hematopoietic progenitor cells. Stem cells (Dayton, Ohio). 2005; 23(9):1324–32.

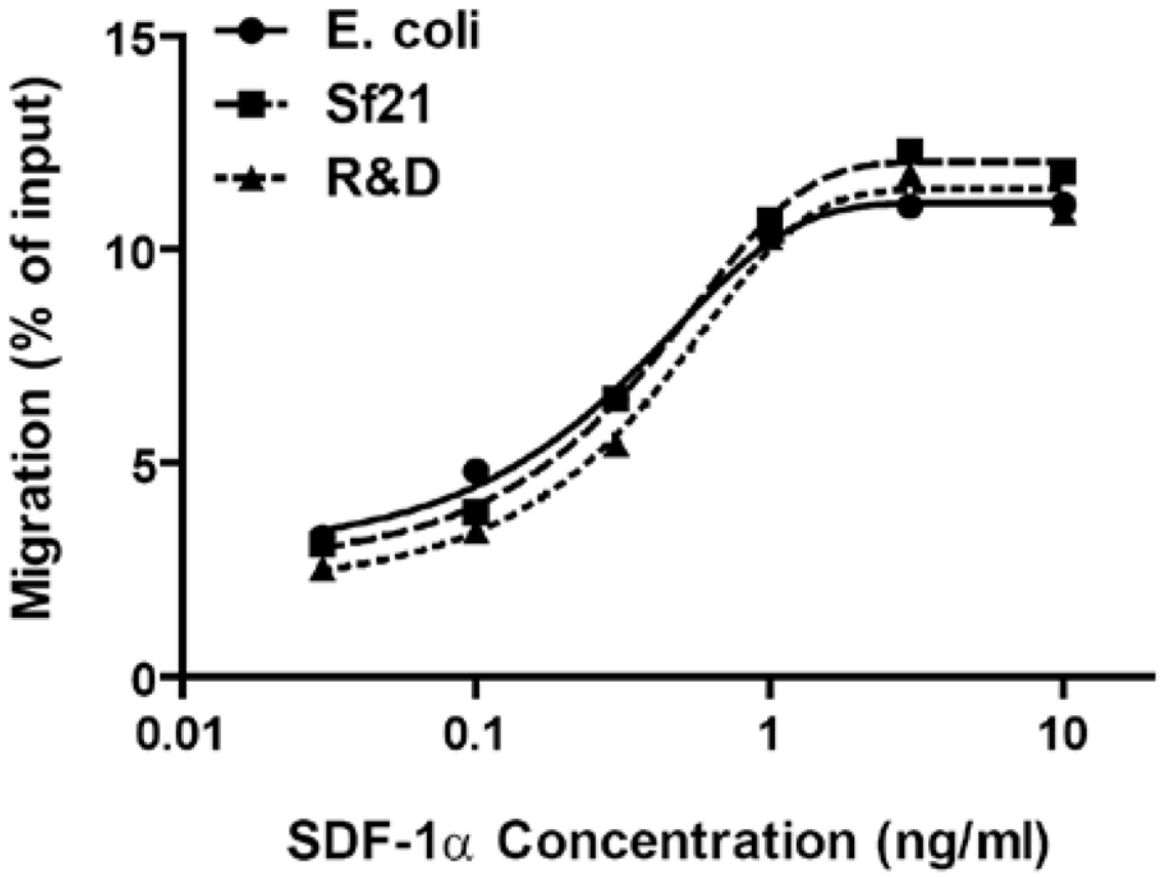

Figure 1. Chemotactic activity of purified recombinant human SDF-1α

Human SDF-1α was expressed in E.coli (circles) and sf21 insect cells (squares), and compared to that obtained from R&D Systems (triangles). Chemotactic activities of the purified proteins were determined by Jurkat cell transmigration assay. Data are presented as the mean of two separate experiments, and are fitted to sigmoidal curves.

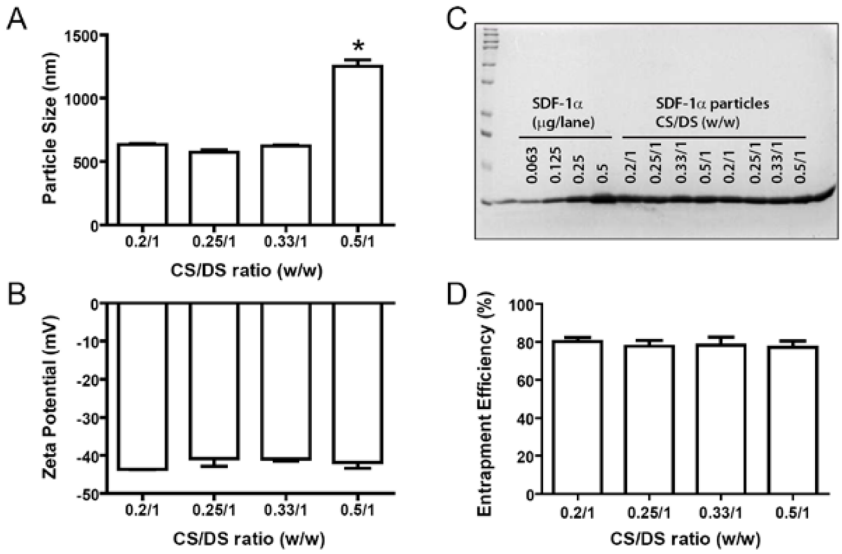

Figure 2. Properties of SDF-1α particles formulated with various ratios of CS/DS

SDF-1α was mixed with the indicated ratios of CS/DS. The resulting particles were assessed for their sizes (A) and zeta potentials (B) using ZetaPALS, and for SDF-1α entrapment efficiency using SDS PAGE (C) followed by band densitometry analysis (D). Panel C, lane 1, MW standards; lanes 3–6, SDF-1α standards; and lanes 7–14, SDF-1α particle suspensions prepared at indicated CS/DS ratios. Data are presented as mean ± SEM, n = 4 – 6 separate particle preparations. *$p < 0.05$ compared to the other groups.

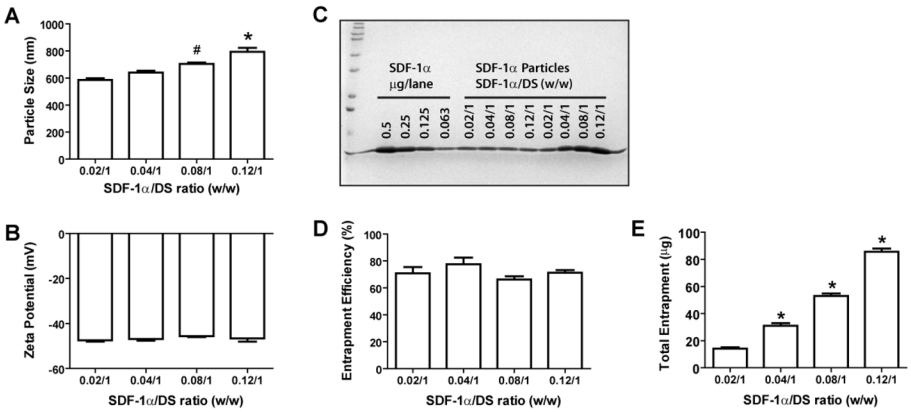

Figure 3. Properties of SDF-1α particles formulated with various SDF-1α-to-DS ratios

Various amounts of SDF-1α were mixed with DS (1 mg) and CS (0.3 mg). The resulting particles were assessed for their sizes (A), zeta potentials (B), and SDF-1α entrapment efficiency (C) and (D). The total entrapment of SDF-1α is shown in (E). Panel C, lane 1, MW standards; lanes 3–6, SDF-1α standards; lanes 7–14 aliquots of SDF-1α particle suspensions loaded in a volume inversely proportional to the indicated SDF-1α/DS ratio (lanes 7–10) or at the same volume (lanes 11–14). Data are presented as mean ± SEM, n = 4–6 separate particle preparations. * $p < 0.05$ compared to the other groups; #, $p < 0.05$ compared to the 0.02/1 group.

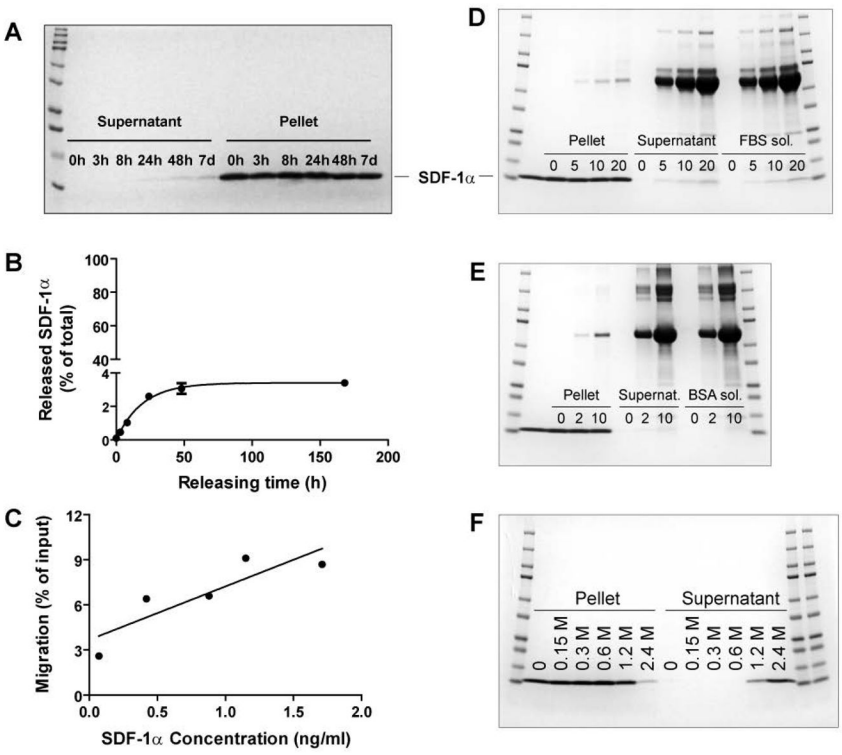

Figure 4. In vitro release of SDF-1α from DS-CS nanoparticles

(A)–(C), SDF-1α NPs were incubated in Release Buffer at 37°C for various times, (A) SDS gel showing the amounts of SDF-1α in the supernatants and pellets at indicated timepoints of incubation; (B) ELISA quantification of the released SDF-1α in the supernatants over time; and (C) correlation of chemotactic activities (by migration assay) and concentrations (by ELISA) of the released SDF-1α in the supernatants. (D) and (E), SDF-1α NPs were incubated at 37°C for 24 h in Release Buffer containing 0, 5, 10, or 20% FBS (D) or 0, 2, or 10 mg/ml BSA (E); Lane 2 shows SDF-1α standard; the remaining lanes (between mw standards) show protein contents in pellets and supernatants of the incubation samples, and in the releasing solutions alone. (F) SDF-1α NPs were incubated in 0, 0.15, 0.3, 0.6, 1.2, or 2.4 M NaCl at 37°C for 30 min; the SDS gel shows the SDF-1α distribution in the pellets and supernatants after the incubation. Data are presented as mean ± SEM, n = 3 separate incubation samples. Gels are representative of three separate experiments.

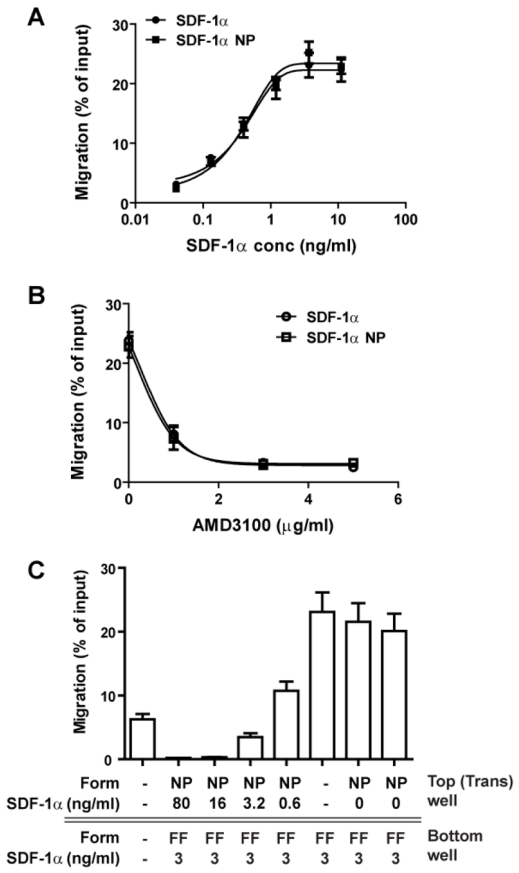

Figure 5. SDF-1α NP exhibits the same chemotactic activity as that of the free form (FF)

(A) Dose-response curves of SDF-1α (circle) and SDF-1α NP (square) in Jurkat cell migration assay. Note that the dose of SDF-1α NP is normalized to SDF-1α content in the NPs. (B) Inhibition assay for Jurkat cell migration: 10 ng/ml SDF-1α or SDF-1α NP was used to induce Jurkat cell migration, which was inhibited by AMD3100. (C) Competition assay for Jurkat cell migration. The assays were carried out by addition of 3 ng/ml SDF-1α (FF) to the bottom wells of the transwell plate, and SDF-1α NPs or control NPs at various concentrations to the top wells. Jurkat cells were loaded in the upper wells.

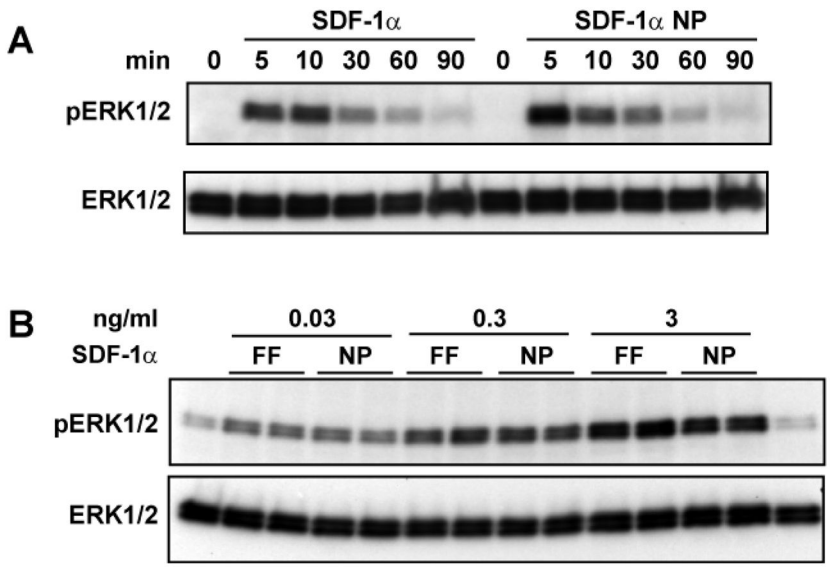

Figure 6. SDF-1α NP activates MAP kinase ERK1/2 similarly as free SDF-1α

Jurkat cells were incubated with 10 ng/ml SDF-1α in free (FF) or NP forms for the indicated time (A) or with the indicated concentrations for 10 min (B). Western blotting analyses were carried out to detect phosphorylated ERK1/2 (pERK1/2) and total ERK1/2 in the cell lysates.

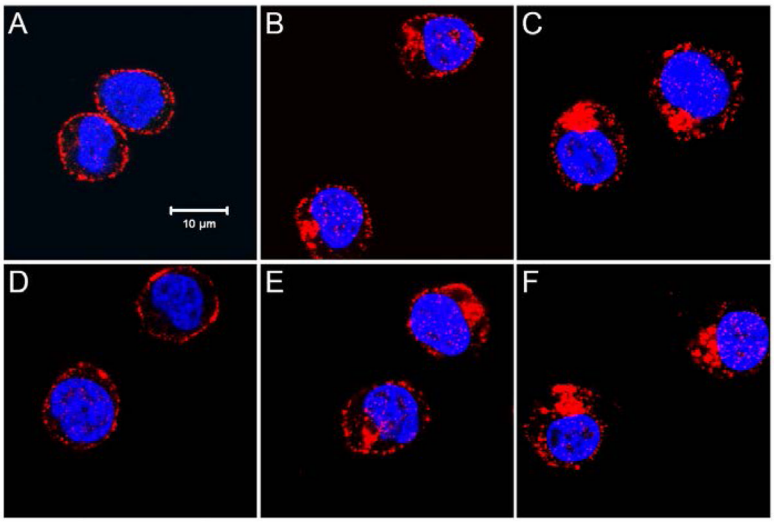

Figure 7. SDF-1α NP activates CXCR4 similarly as free SDF-1α

Jurkat cells were incubated in culture medium for 30 min with nothing added (A), or with addition of SDF-1α at 1 ng/ml (B) or 10 ng/ml (C), control CS-DS nanoparticles (D), and SDF-1α NP at 1 ng/ml (E) or 10 ng/ml (F). Cells were subsequently fixed, permeabilized, stained with APC-conjugated anti-CXCR4 antibody (shown in red), and counterstained with DAPI (a nuclear dye, blue). Confocal microscopy images were taken at the middle plane (z-series) of the cells. Bar = 10 μm. Note that activation of CXCR4 is manifested by internalization and aggregation of the receptor, with SDF-1α and SDF-1α NP inducing similar effects.

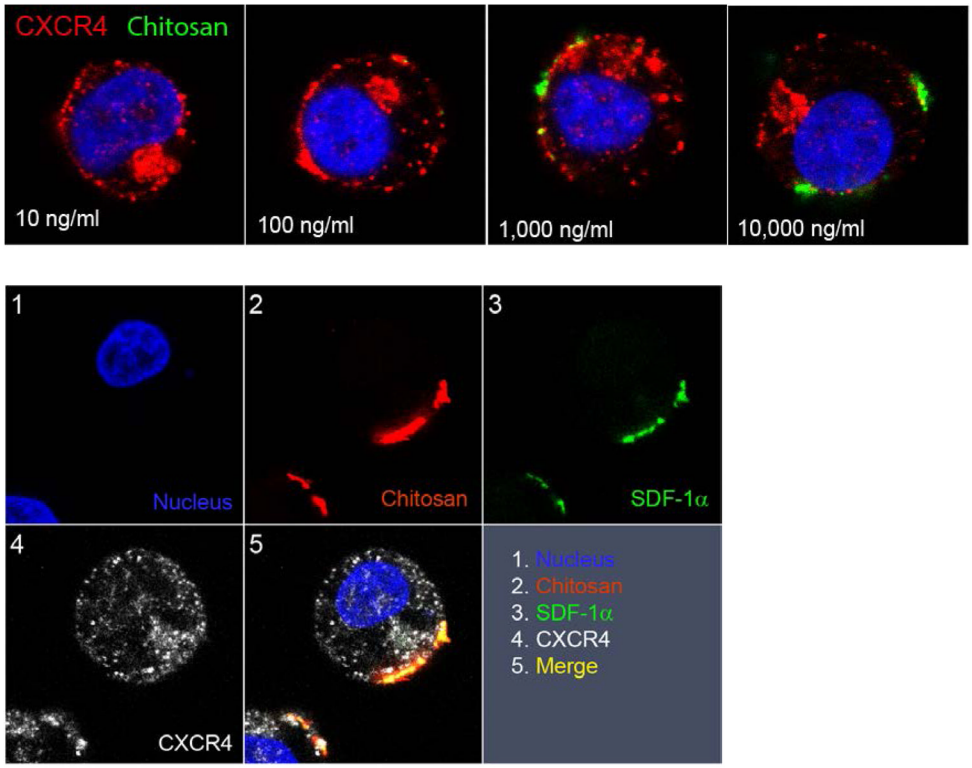

Figure 8. Confocal images showing the localization of *SDF-1α* NPs after incubation with Jurkat cells

Top panel, cells were incubated with various amounts of SDF-1α NPs (normalized to SDF-1α concentration) containing FITC-chitosan (green), and were stained for CXCR4 (red) and nucleus (blue). Lower panel, cells were incubated with 5,000 ng/ml SDF-1α NPs containing rhodamine-chitosan and FITC-SDF-1α. The cells were stained for CXCR4, FITC, and nucleus before imaging. The split panels show the individual and merged images of the fluorescence-stained molecules.

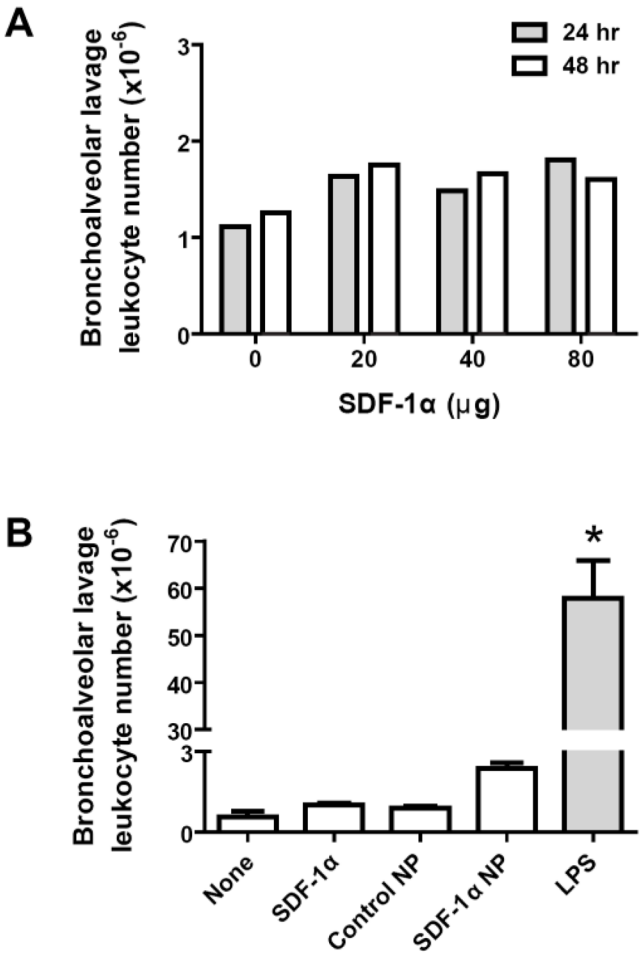

Figure 9. No significant inflammatory responses are found in rat lungs treated with SDF-1α or SDF-1α NP

(A) PBS solutions containing 20, 40, or 80 μg of SDF-1α were aerosolized to the lungs of rats. At 24 hr (filled bar) and 48 hr (open bar) after delivery, bronchoalveolar lavage (BAL) was performed. Leukocytes in the lavage fluid were pelleted and counted. The total number of cells from each rat was plotted. Data are shown as the mean of the counts from 2 rats per group. (B) PBS solutions containing 15 μg SDF-1α or SDF-1α NP, control NP (without SDF-1α), or 200 μg lipopolysaccharide (LPS) were aerosolized into the lungs of rats. At 24 hr (filled bar) and 48 hr (open bar) after delivery, BAL was carried out as described above. Data are presented as mean ± SEM, n = 3 rats per group, $*p < 0.05$ compared to the other groups.

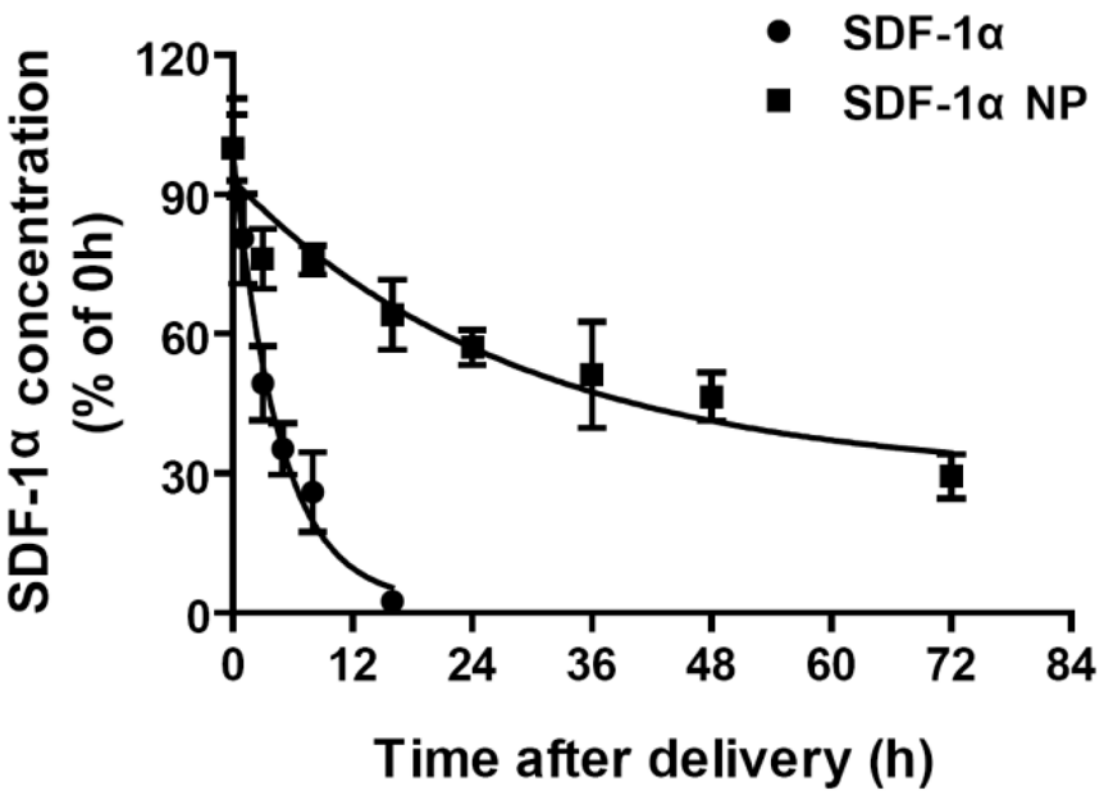

Figure 10. SDF-1α NP exhibits greater retention time in the lung compared to SDF-1α

SDF-1α (20 μg) and SDF-1α NP (13 μg SDF-1α content) were aerosolized into the lungs of rats. At the indicated timepoints, lung tissues were harvested and homogenized. The concentrations of SDF-1α in the supernatants of the homogenates were determined by ELISA, and plotted as percentages of that in the tissue harvested at 0 hr. Data are presented as mean ± SEM, n = 4–8 rats per group. Data are fitted to monophasic exponential decay curves.

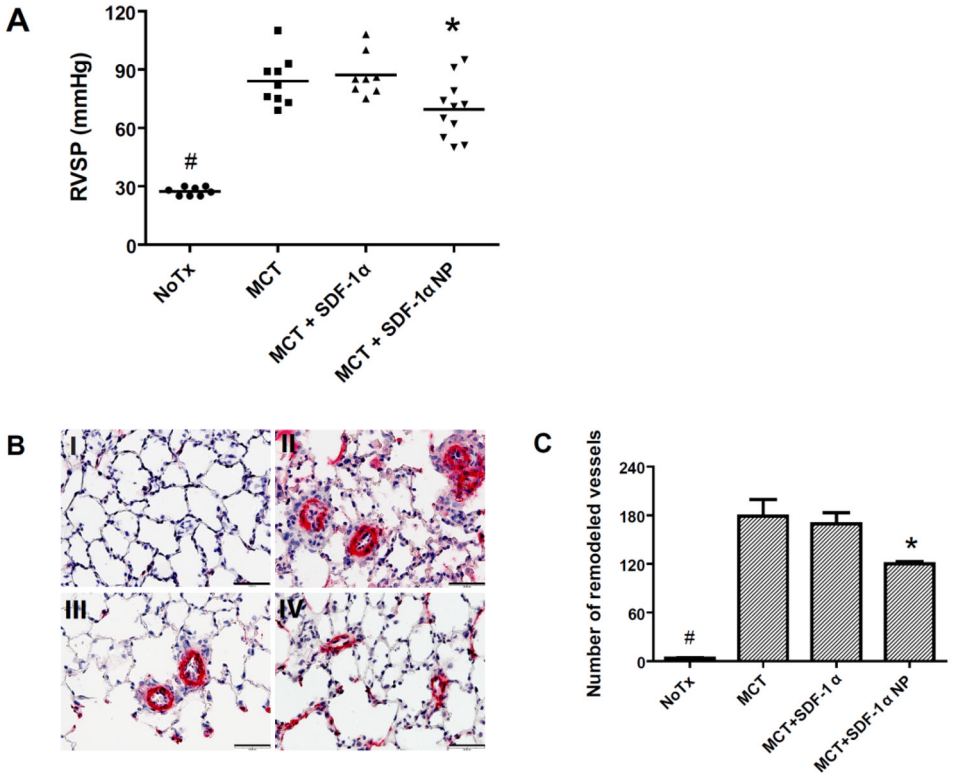

Figure 11. SDF-1α NP but not SDF-1α reduces monocrotaline-induced pulmonary hypertension in rats

Rats were injected with monocrotaline (MCT, 50 mg/kg, i.p.) at day 0. At day 3, 15 μg SDF-1α or SDF-1α NP were aerosolized into the lungs of the rats. At day 21, right heart catheterization was performed in the rats followed by lung tissue harvest. (A) right ventricular systolic pressure (RVSP) measurements of the rats. Data are presented as individual measurement in each rat, as well as the mean of each group; n = 8–11 rats per group, *$p < 0.05$ compared to the MCT or MCT + SDF-1α group; #, $p < 0.05$ compared to the other groups. (B) Representative tissue sections with alpha smooth muscle actin staining obtained from rats with no treatment (I), with MCT (II), MCT + SDF-1α (III), or MCT + SDF-1α NP-treatment (IV). Bar = 50 μm. (C) Counts of alpha smooth muscle actin-stained vessels with diameter <50 μm in the entire lung section from the rat samples marked in red shown in panel A; n = 4 per group, *$p < 0.05$ compared to the MCT group; #, $p < 0.05$ compared to the other groups.

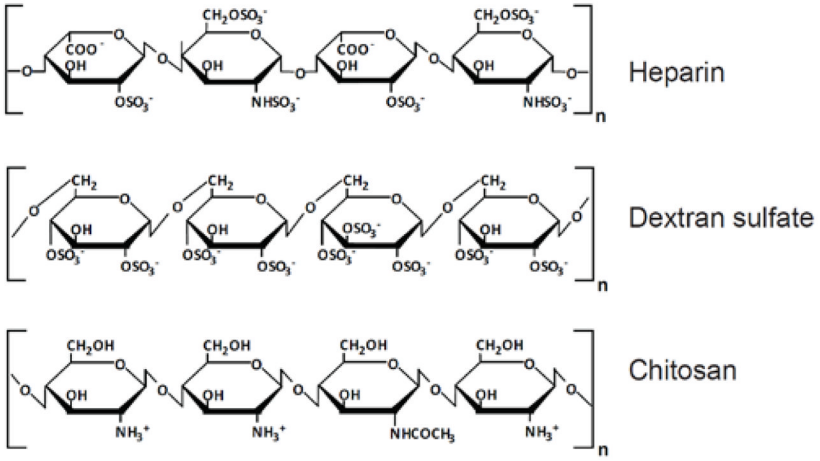

Figure 12. Generalized structural units of glycans

Heparin, (1–4)-linked 2-sulfo-α-L-iduronic acid and α-D-N-sulfoglucosamine-6-sulfate; Dextran sulfate, (1–6)-linked α-D-glucose sulfate (5% with α-1,3 linkage); Chitosan, β-(1–4)-linked D-glucosamine (deacetylated unit) and N-acetyl-D-glucosamine (acetylated unit).